ICAS 2021 SHANGHAI
International Council of the Aeronautical Sciences
32nd Congress of the International Council of the Aeronautical Sciences
September 6-10, 2021
Pudong Shangri-La, Shanghai, China

TEAM S55: 1:8 SCALE “REPLICA” OF THE SIAI-MARCHETTI S55X

L. Di Ianni[1], L. Loiodice[1], D. Celestini[1], D. Tiberti[1], C. Baldon[1], P. Iavecchia[1], A. Saponaro Piacente[1], M. Prodan[1], S. Grendene[1], B. Barberis[1] & L. Santoro[1]

[1]Department of Aerospace Engineering Politecnico di Torino,

Corso Duca degli Abruzzi 24, 10129, Torino, Italy

Abstract

The purpose of this work is to show the engineering approach and the technical contents of an aeronautical design activity performed by a student team, the “Team S55”, a group of young engineers and students organized within the Department of Aerospace Engineering (DIMEAS) of “Politecnico di Torino”, in order to be able to engage students in extra-curricular activities, which are a source of experience and learning.

The current goal of the team is to design and realize a 1:8 scale and flying “Replica” of the SIAI-Marchetti S55X. Afterwards the members focused on Weight and Balance analysis that evaluated the inertial properties of the scale model and the S55-X in order to have an accurate prediction of the weight and to match the position of the center of gravity of the 1:8 model. For Aerodynamics and Flight Mechanics, the analysis started with the study of both the model’s and the original’s aerodynamic curves obtained using AVL (Athena Vortex Lattice), an open-source program developed by MIT. Then, the aerodynamic analysis was deepened through CFD simulations using STAR CCM+ in order to correct the aerodynamic curves, to study the cruise phase and to obtain the pressure field on the seaplane.

The structural analysis was made using the Finite Element Code ANSA, developed by BETA CAE System. The structure of the model aircraft was divided in major components and, for each part, it was performed a CAD modification for the structural idealization, interface and FEM geometry definition, mesh preparation, material properties definition, modal analysis, loading result’s analysis and propose modifications on the components.

Keywords: Model aircraft, Seaplane, Flight Mechanics, Aerodynamics, FEM

1. History of “Team S55”

The “Team S55” was born in February 2017 from a small group of students of the “Politecnico di Torino” driven by the passion for aeronautics and with the aim to help the “Replica 55” group in the design of a flying “Replica” of the SIAI-Marchetti S55X.

Over time, the activities within the team, first focused on the creation of CAD models and on flight mechanics and structural analysis, have increased in number allowing students to approach a 360° aeronautical project. In fact, members have the opportunity to increase their knowledge, studying and putting into practice concepts related also to aerodynamics and hydrodynamics (by CFD analysis), systems and propulsion (electric ones), dynamic analysis of water impact (numerical simulations and experimental tests), materials (modern like composites) and production technologies (innovative like Additive Manufacturing). In addition, some of the students, who are distinguished by their commitment and dedication to the project, can participate in national and international events and internship programs.

It is evident that the real driving force of the team is the possibility of living an integrated design experience between the various disciplines not only technical and managerial but also of interpersonal relationships, as if it were a matter of anticipating a company simulation, in the form of “training on the job”. The whole group is configured and operates as an integrated technical design office, which in any case has not only design, calculation and verification capabilities, but also implementation skills and the possibility of setting up experimental ground and flight test.

The S55 also has a strong link with the “Politecnico di Torino”. Prof. Giuseppe Gabrielli, in fact, designed a metal version of the S55X seaplane becoming the first italian model of an airplane made of metal.

2. CAD Model

The current goal of the team is to design and realize a 1:8 scale and flying “Replica” of the SIAI-Marchetti S55X, a symbol of the remarkable aeronautical know how reached in Italy during the ‘20s and ‘30s. This goal has received great enthusiasm from team members that focused their work on a careful analysis of the original plans to design the model described in this chapter.

2.1 Analysis and Simplification of CAD drawings

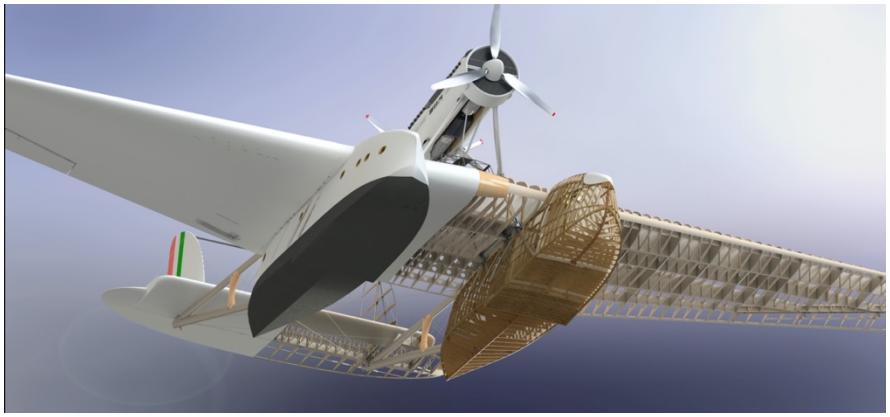

Figure 1 – A rendering of the “Replica 55” [1]

The project began in collaboration with “Replica 55”, an historical research group whose members are professionals of the aeronautical sector. Their goal is to design, build and fly the faithful replica of the SIAI Marchetti S55X seaplane. Thanks to their meticulous CAD drawings (figure 1) and to some historical documents [2] and [3], the team managed to elaborate Marchetti’s structural and assembly choices.

The first step of the team’s work was to analyze the “Replica 55” CAD and then to proceed with its simplification, which was the starting point for the design of the 1:8 scale model (figure 2), this complex work needed some specific working process and design choices:

1. Trying to maintain the division in parts of the original plane was one of the main requirements, as it made possible to use a similar, but simplified, structural scheme;
2. Removing all the unnecessary non-structural components was mandatory;
3. Making the model as light and simple to build as possible, in order to participate to RC model competitions which are restrictive on the MTOW;
4. Basing the structure on the use of modern composite materials;
5. Reducing the number of structural elements to better fit the smaller scale (1:8).

Figure 2 - A render of the CAD model of the Team S55 model aircraft

The team started its design process with the most important part of the seaplane, the wing.
In the original aircraft, this element (24 meters long) is divided into three sub-elements (one central section and two half-wings) onto which all the other parts are attached. The original plane was all made from wood and had a very complex internal structure made of hundreds of parts.
As to maintain the main characteristics and external shape of the original aircraft, even in the case of our scale replica, the wing plane was still divided in 3 parts which differ in the internal structure, widely simplified. In fact, the work was focused on eliminating non-structural elements and simplifying the remaining ones.
For example, the original plane fitted the cockpit and lots of flight systems in the wing, while we only had to route some cables and other electrical flight control components, which led to the removal of a large number of internal structures.
We based our design on a simpler two spar (main front and secondary rear, carbon composite) and ribs (fiberglass-foam sandwich).

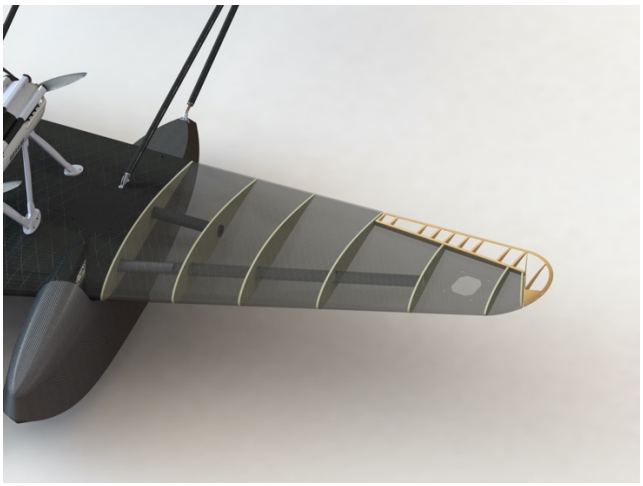

Figure 3 - Detail of the model aircraft wing

- **Main Spar**: it’s made by a cylindrical element (internal diameter = 30mm) running along the entire wing and as previously described is divided in 3 parts. This allow the disassembly and transportation of the model. Its thickness varies in function of the load distribution – *better explained in the structural analysis chapter* – to get a lighter but still stiff component, as its purpose is resisting to bending loads and aerodynamic forces that the seven ribs of the half-wing transmit from the skin to the spars. The three parts are mounted with additive

manufacturing realized joining bars (bayonets), as seen in blue in the figure 4, which provide the correct dihedral and sweep angle (figure 5), dihedral angle = 175,2°, sweep angle = 167,6°.

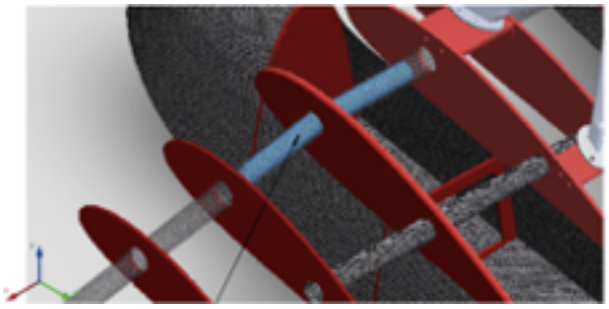

Figure 4 – Bayonet

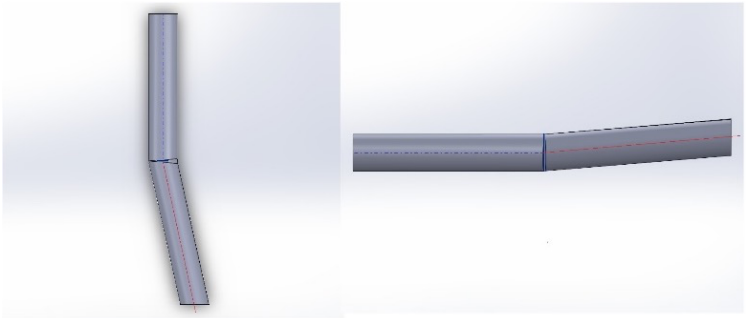

Figure 5 – Sweep (left) and dihedral (right) angles of the bayonet

- **Rear spar:** this secondary spar, reacting wing torsion was realized as the first one, but features a shorter length, as it ends at the beginning of the half-wings. The joint between this spar (attached to the central wing section) and the half wings is made by inserting a section of carbon tube (internal diameter 30 mm) into which the tip of the spar slides.
- **Ribs**: the plane features a total of 20 ribs, 7 per half-wing and 6 on the central wing plane, those are all realized with the same material and techniques.
    - *Half-wing:* only the first 5 ribs of the wing are bonded to the main spar, which sets in specifically sloped holes to guarantee a tight fit of the swept spar. The first 2 ribs also feature holes to fit the short carbon tube section that allows the rear spar from the central plan to slide in. The central 3 ribs are all fitted to the main spar and are designed to receive a great part of the wing loads. The last 2 ribs have only a wing shape purpose because the stress level in the area is quite low.
    - *Central Plane:* the 2 external ribs interface with the half-wing and together with the 2 that precede them, are positioned so that they coincide with the hull sides. The 2 innermost ribs, together with the latter, instead transmit the loads coming from the overlying engine truss and the rear tail booms, from the skin to the two spars.
- **Skins:** the entire wing is covered with carbon fibre skins, specifically laminated to reproduce the wing profile shape.
- **Ailerons:** the aileron, due to aesthetic needs, was realized with classical modelling techniques, from balsa wood and light plywood.

Another critical aspect of the project was the construction of the two hulls, due to their particular shape, which is a concave-convex profile that changes throughout the length and is divided by a “redan” (step, placed on the bottom of the floats of a seaplane, to decrease the resistance to motion to the advantage of speed). This time we went more radical with the simplification process, leaving only the carbon fibre external skin, and 4 frames deputed to maintain stiffness and shape, always taking care of the

waterproofness of the component. The formers also provide an attachment point for the joints with the other parts of the plane which we are going to describe in the following section.

Figure 6 - Hull and attacks with the aircraft's wing plane

As to the joining all the parts of the plane together, we based on the original division criteria with the idea to maintain the original-scaled interfaces between hulls and the wing. After many problems raised, such as:

1. Batteries housing impermeability, which mean a waterproof hull and the necessity to route the batteries cables to the engines without any water infiltration;
2. Hull-wing alignment necessity;
3. Different material realization criteria (our model is not in wood);

We decided to change the joints configuration. The final decision was to realize an aluminium rod in the front part of the central wing and an aluminium tube in the rear part, which together provide the correct alignment of the hulls. Moreover, the main joints were realized with an aluminium profile. Their shape is square so to allow the cable route, preserving the hull impermeability as shown in figure 6.

Concerning the control surfaces, the aileron, the tail was made of balsa with an oracover® skin. We decided to use these materials due to low weight and esthetical requirements. The only structural part done with different material is the rib interfacing the tail, the tail booms and the vertical stabilizer, which is a 3D printed reinforced plastic part (see figure 7). The tail structure is jointed to the main fuselage via a carbon rod structure, which takes inspiration from the original design but results in a cleaner and lighter design. Those parts are all jointed using some special shaped attachment elements, whose design is very similar to the original ones. Those components are realized with advanced technologies such as metal additive manufacturing, using a light and stiff aluminum alloy.

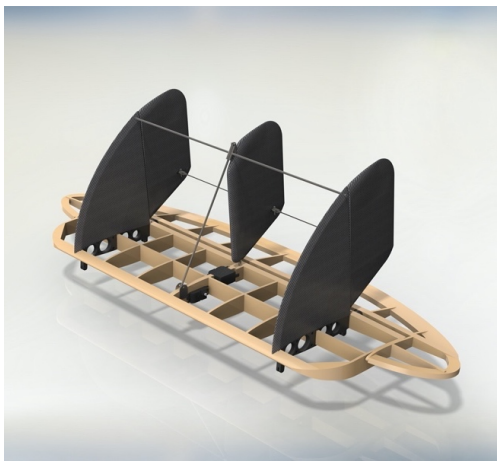

Figure 7 – Tail of the model aircraft

Last but not least, our work focused on one of the most distinctive parts of the plane, the engine mount, starting from the original CAD drawing of the piece, the 1:1 assembly is made of many parts including metallic parts, wood parts, bolt and that made it complex and very difficult to reproduce in a 1:8 scale. We decide to use additive manufacturing, a SLM (selective laser melting) process. The first things we have done was the simplification of the geometry of the assembly to obtain a printable part. We start from the original CAD removing all the features that were not reproducible in a 1:8 scale. The base plates are also adapted to better connect the mount to the wing, in particular they are too small when scaled so they must be enlarged in order to use M3 bolt to attach the two pieces. The completed CAD model was printed on a Print Sharp 250 machine available from one of our sponsors (Ellena-SPEM company) and all the pieces were manufactured in one print job. In figure 8 the four pieces printed, and the final assembly are shown.

Figure 8 - Legs of the engine mount made of AM (left), CAD of the engine mount with fairing (right)

2.2 Materials choice

Due to the F4C regulation [4] that imposes a 15Kg on empty weight, the choices of the materials are limited to the use of very light materials such as carbon fiber, rigid foam, fiberglass and balsa wood. For the main parts of the airplane such as wing and hull the choice was carbon fiber for skin and sandwich ribs (rigid foam and fiberglass face), this choice is made taking into account several factors, some of them not of technical nature, first of all the students interest in learning to use advances materials.

On the other hand, there are strong technical reasons. The manufacturing of wood pieces by students with little or none previous experiences in manufacturing this components could result in poor tolerances and imperfection that could led to catastrophic event during flights. The plane also need to be sealed especially on hulls because they contain batteries and they are in the water during takeoff, landing and parking phase. Also, if wood is not accurately painted and treated it tends to absorb moisture and this could change mass distribution, cause distortion and at last rotting.

The weight factor, anyway, is the most important, so we have done a selection based on the criteria of material indexes.

T700		E/ρ	**Balsa**		E/ρ
$E_{11}[GPa]$	130	0,083	$E_{11}[GPa]$	3,3	0,0021
$E_{22}[GPa]$	10,3	0,0065	$E_{22}[GPa]$	0,27	0,00017
$G_{12}[GPa]$	6,5	0,0041	$G_{12}[GPa]$	0,14	8,92E-05
$\rho\left[\frac{kg}{m^3}\right]$	1570		$\rho\left[\frac{kg}{m^3}\right]$	1000	

Table 1 – Material properties and weight factor

From the table we see that, as expected the carbon fiber wins. Note that in the table the material properties of the carbon are lower than the nominal found in literature [5] to take care of some manufacturing defect that could be present in the final pieces.
In fact, for the curing of the laminate we use 3D printed tools [6] and [7], this tool made by us are not suitable for autoclave curing (they are made of PLA that has a T_g of 60 °C) so the final laminate properties cannot be compared to the other manufactured with autoclave.

3. Weight and Balance analysis

3.1 Inertial properties of the scale model

The Weight and Balance analysis studied the inertial properties of the scale model and the S55-X to comply with the limits imposed by static stability and try to evaluate the weight and the position of the 1:8 model center of gravity.
This analysis was conducted together with the development of the CAD model and supported the creation of the CAD itself, checking step by step the model total mass and position of the center of gravity. After the creation of each element CAD model, SolidWorks features were used to obtain its mass, CG and moments of inertia about axis parallel to the global system shown in figure 9 (where plane O_{xz} is coincident with the symmetry plane of the vehicle and the y axis completes the right-handed tern). Afterwards, the entire model properties were derived using a spreadsheet. Once the CG position of the whole plane was evaluated, the Huygens-Steiner theorem led to the calculation of the model moments of inertia relative to a reference system aligned with the aforementioned global axes but centered in the model CG itself.
The analysis was useful to understand how to modify the position of the model CG shifting internal components, such as batteries and servomotors. A simple but useful graphical tool used to provide an effective representation of the overall inertial characteristics is shown in figure 9. The graph contains not only the position of both the elements and the entire plane CG but also the limits regarding its position along the x-axis imposed by longitudinal static stability.

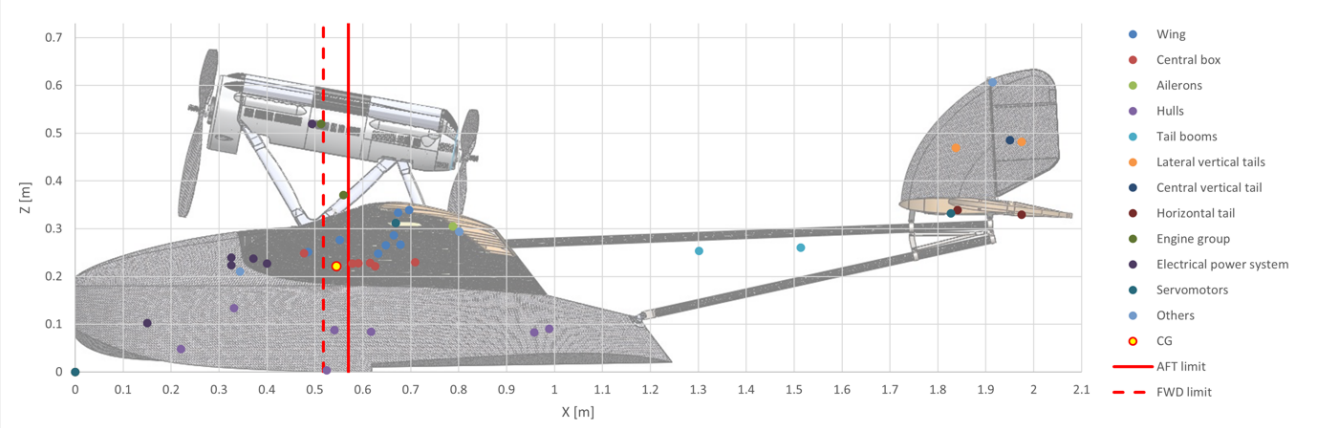

Figure 9 – Position of the CG of all the model elements and limits on the plane CG position

3.2 Floating characteristics of the model

One of the analyses that exploited the inertial features of the plane was the study of the seaplane floating characteristics. The global mass and the CAD model of the hulls were used to find the waterline and check the static floating stability of the scale model in presence of roll or pitch angles. The scale model waterline calculated resembles the original one, as depicted in figure 10.

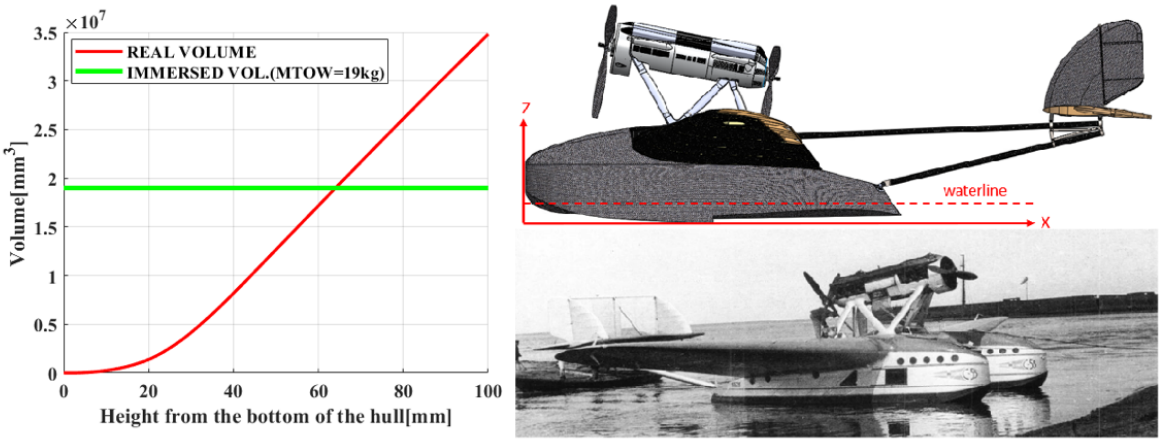

Figure 10 – Immersed volume-height, CAD representation of the scale model and historical photo of the original plane

4. Aerodynamics and Flight Mechanics

4.1 Preliminary aerodynamic analysis using AVL

The analyses started with the study of both the model’s and the original’s aerodynamic curves obtained using AVL (Athena Vortex Lattice), an open-source program developed by MIT [8]. AVL is a program for the aerodynamic and flight-dynamic analysis of rigid aircrafts that employs an extended vortex lattice model for the lifting surfaces, together with a slender-body model for fuselages. The geometry 1:8 model built in AVL appears in figure 11: the AVL model is not as detailed as the CAD one, but it contains the hulls and each lifting surface of the vehicle.

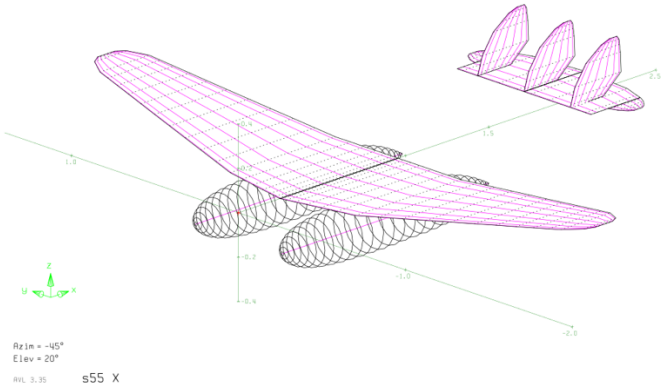

Figure 11 – Geometry 1:8 model created in AVL

4.2 Aerodynamic analysis using CFD

A more detailed aerodynamic computation has been conducted for the model aircraft using the ANSA and Star CCM+ [9] computational fluid dynamics software. This allowed to obtain a more precise set of data than the ones computed with the non-viscous flow in the AVL software. A series of simulations of the model aircraft in cruise flight configuration and at various angles of attack has been run, in order to visualize the lift and drag polar curves of the aircraft and to compare the collected data with the ones obtained with the use of the AVL software coupled semi-empirical formulae.

The CAD geometry used for these analyses is the same one used for the calculation with the AVL software, presenting the main airframe of the aircraft, the wings, the tail and the two hulls, as shown in figure 12.

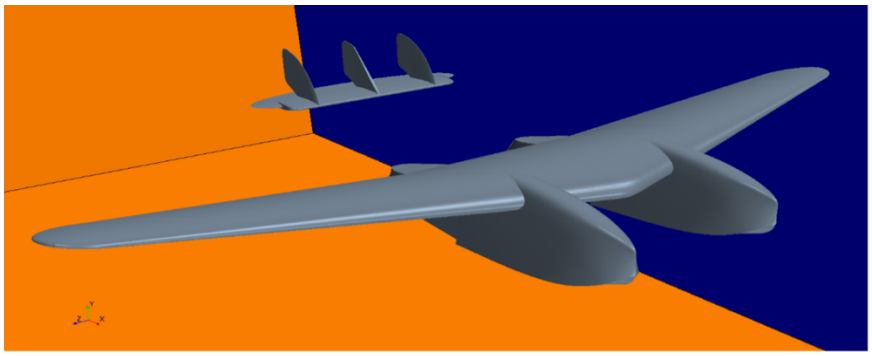

Figure 12 – CAD geometry for the computational fluid dynamics simulations

This geometry was imported into the ANSA software, where a surface cleanup was executed, in order to prevent the generation of invalid mesh elements, usually found near the trailing edges of the lifting elements or near the junction points of the rudders and the stabilizer. Then, using the meshing software, the surface and volume meshes were generated. Figures 13 and 14 show a detail of the surface mesh created on the aircraft.

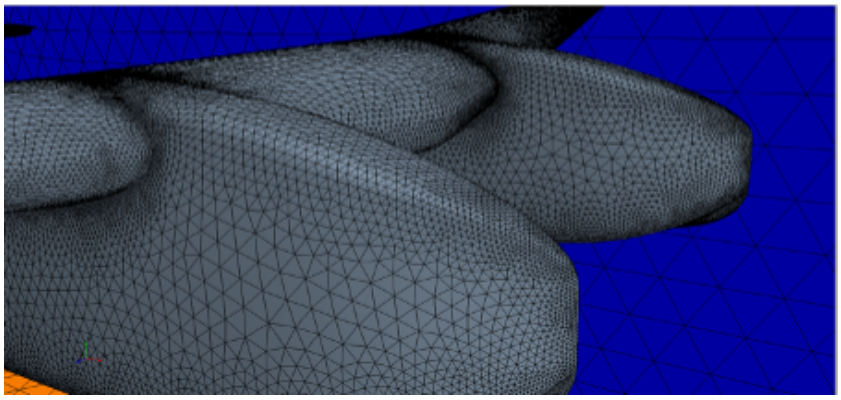

Figure 13 – Detail of the surface mesh on the hulls of the model aircraft

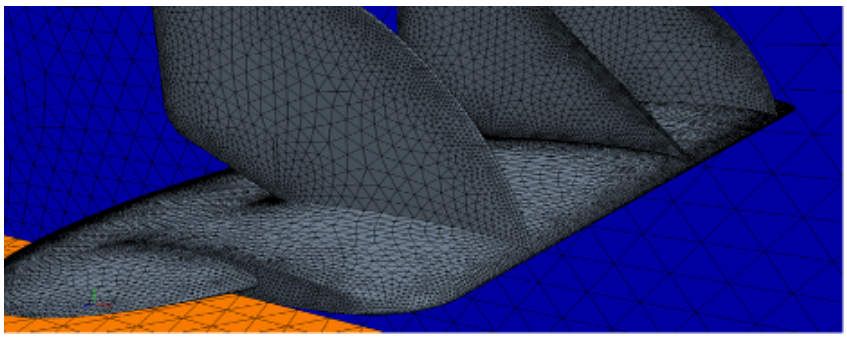

Figure 14 – Detail of the mesh on the tail of the model aircraft

After the generation of the volume mesh on the whole domain around the geometry, the mesh was imported in Star CCM+, where the appropriate physics models were assigned to the domain, according to the parameters of low Mach number and high Reynolds number. The simulations were made considering the fluid domain as composed of an ideal gas, therefore taking into account of the compressibility of the fluid. Moreover, the high Reynolds number calculated ($1.03 \cdot 10^6$) suggested the need of a turbulence model to take into account of the viscosity changes and the relative effects in the fluid domain. For this purpose, the two-equation K-Epsilon turbulence model was chosen. Ultimately, the simulation was launched to calculate the lift and drag coefficients of the model aircraft. Figure 15 shows a scalar scene of Star CCM+ depicting the obtained pressure field around the aircraft, and figure 16 depicts the related velocity field.

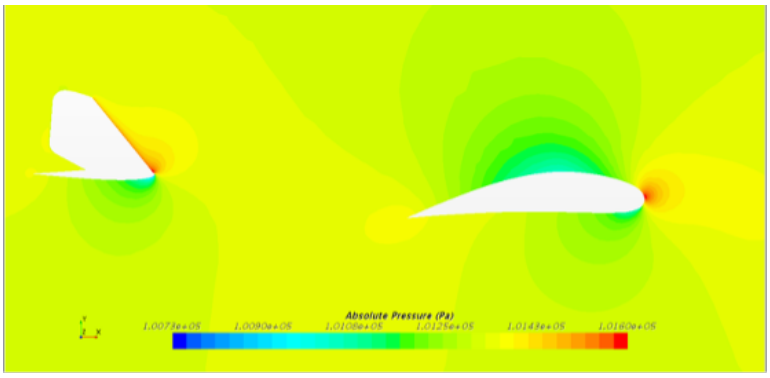

Figure 15 – Absolute pressure field

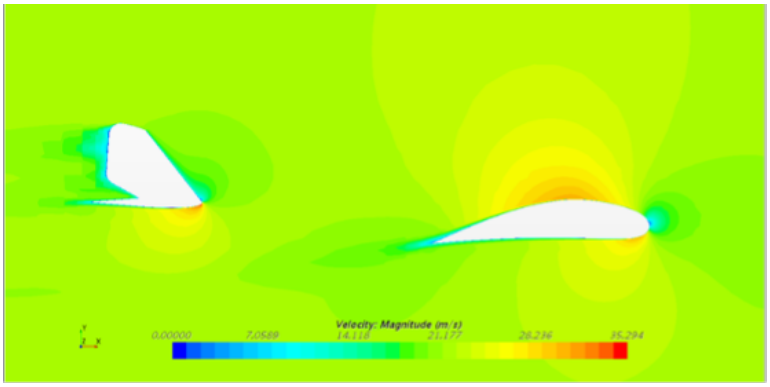

Figure 16 – Velocity field

Having verified the correctness of the results obtained for the first analysis, a set of simulations was subsequently completed, in order to simulate the flight at a range of angles of attack varying between –10 and +10 degrees. Finally, the collected data were put together to generate the polar curves for the model aircraft.

The lift coefficient Vs – drag coefficient polar was then compared to the one previously obtained with the AVL software and the semi-empirical formulae. A very good correspondence between the two curves can be seen.

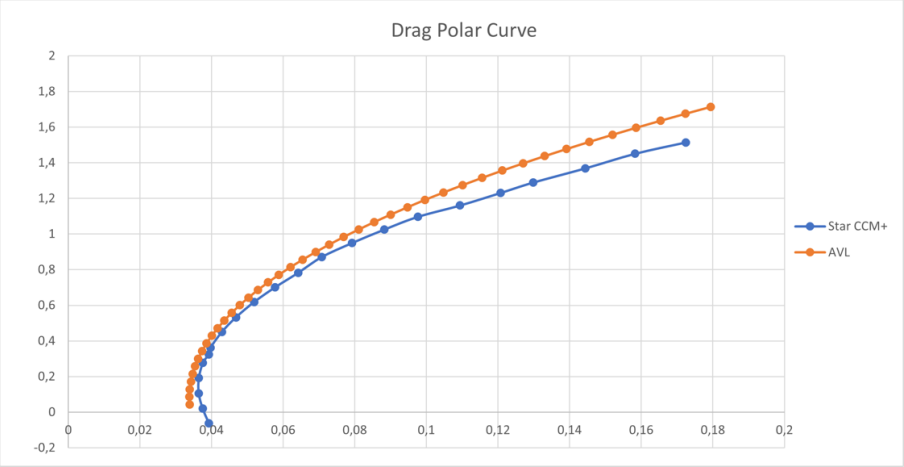

Figure 17 – Drag Polar Curve

4.3 Static stability analysis

Once the aerodynamic characteristics of the scale model were calculated, the static stability of the plane was checked in MATLAB environment. The first step of the process was to import the aerodynamic

curves obtained and evaluate those aerodynamic derivatives which are fundamental to achieve static stability. The results obtained are listed below.

- $C_{M\alpha} < 0$ granting longitudinal static stability, with parabolic trend;
- $C_{L\beta} < 0$ and $C_{N\beta} > 0$ granting lateral and directional static stability, with linear trend;

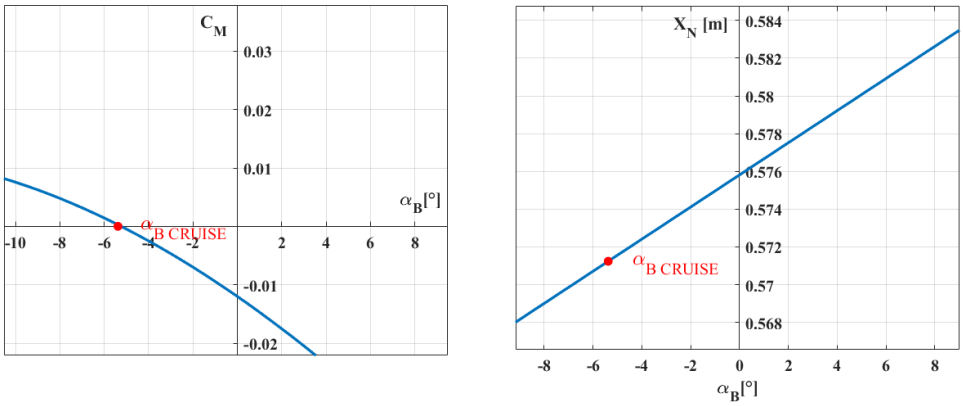

Figure 18 – Pitching moment coefficient (left) and aerodynamic center position (right) in relation to angle of attack

In figure 18, the symbol α_B represents the angle of attack of the vehicle measured w.r.t. (with respect to) the fixed body axes, centered in the model CG and following the standard orientation: X forward, Z down and Y in order to complete the set of axes. It is important to notice that, although longitudinal static stability requirement $C_{M\alpha} < 0$ is met, $C_{M\alpha}$, cannot be considered constant as the angle of attack varies. This characteristic causes the position of the aerodynamic center X_N (expressed in Weight and Balance global axes in figure 18) to shift as α_B varies. Furthermore, it is noticeable that the trimmed flight condition can be reached without elevator deflection when the angle of attack measured w.r.t. the body axes is $\alpha_B = -5.4°$. This flight configuration, considered as the cruise one, finds confirmation in historical photographs, too.
This initial analysis did not include the pitching moment introduced by thrust, which is an important factor particularly for seaplanes that have the propeller far from the water and from the CG of the plane. This pitching moment is related to the thrust, which varies as flight condition changes to maintain trim. However, the flight condition itself depends on the value of angle of attack and deflection of the elevator, both determined by the thrust pitching moment. The iterative model merging the aerodynamic and propulsive contributions to calculate the trim condition highlighted the importance of the horizontal tail pitch, the value of which determines the elevator deflection necessary to balance the moment caused by thrust. To achieve the same cruise flight condition even considering the thrust negative pitching moment we decided to have the possibility to vary the pitch angle of the tail before take-off, the nominal value of which was calculated as $i_t = 2.5°$ (pitch reduction of about 1° w.r.t. the original aircraft).

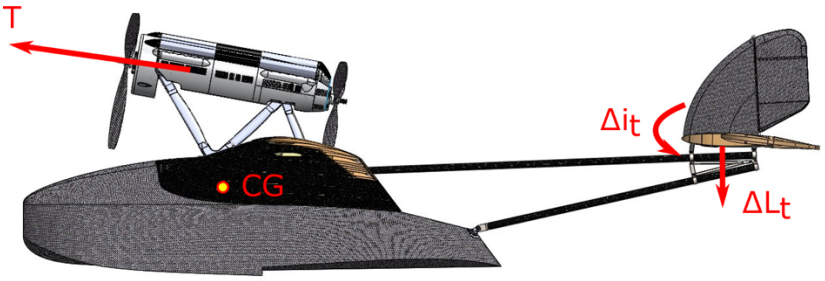

Figure 19 – Tail pitch correction Δi_t to balance the negative pitching moment caused by thrust T

The MATLAB model built to merge aerodynamic and propulsive contributions was, then, used to study different phases of the flight, such as straight horizontal or climb trimmed flight and banked trimmed

flight. Figure 20 shows some examples of the graphs obtained studying climb trimmed flight with different values of γ, the flight path angle.

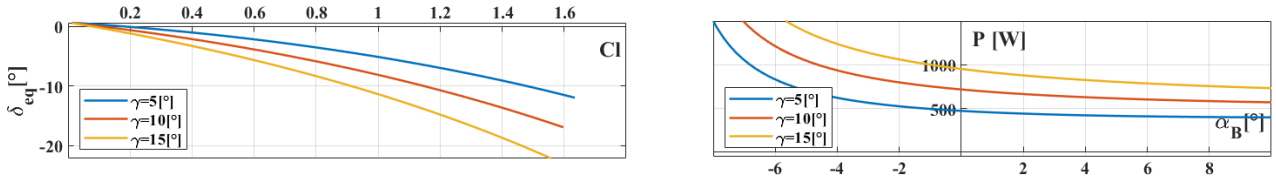

Figure 20 – Results of the analysis of trimmed climb flight with three different values of flight patch angle γ

4.4 Dynamic stability analysis

The Dynamic Stability analysis of the model started with an eigenvalue analysis implemented in MATLAB environment. This analysis allowed us to understand the dynamic behaviour of the model through a linearization of its aerodynamic and control derivatives around a chosen trimmed flight configuration, such as the cruise one. The state-space is represented in the form:

$$\{\dot{x}\} = [A]\{x\} + [B]\{u\}$$

where $\{x\}, \{\dot{x}\} \in \mathbb{R}^n, \{u\} \in \mathbb{R}^m$ are respectively the state vector, its derivative and the input vector, while $[A] \in \mathbb{R}^{n\times n}, [B] \in \mathbb{R}^{n\times m}$ are the state and input matrices. The dynamic stability of the free system ($\{u\} = \{0\}$) response to a perturbation around the trimmed flight condition depends on the eigenvalues of the state matrix $[A]$. Figure 21 depicts the trend of the 1:8 model short period and phugoid, the two typical modes characterising a plane’s longitudinal motion.

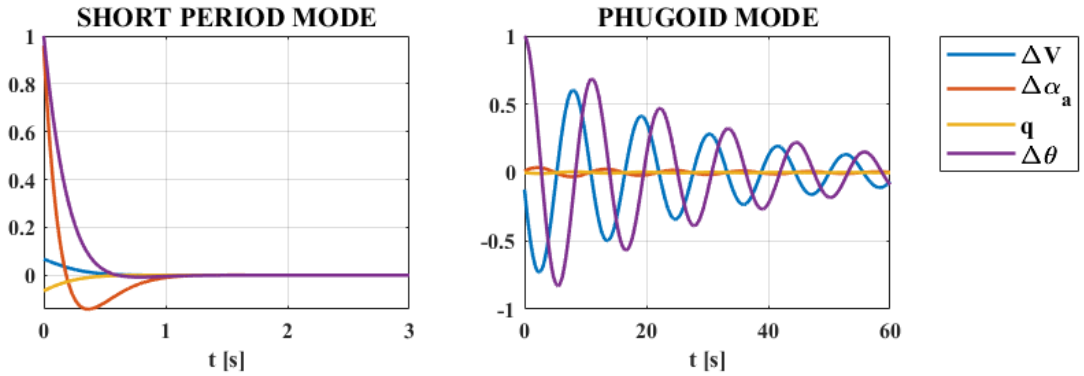

Figure 21 – Normalized response of the scale model to a perturbation acting on the longitudinal plane

Once the both the longitudinal and lateral-directional dynamic stability of the model was checked in some representative flight configuration, the dynamic response to a command was evaluated. For this purpose, a flight simulator of the 1:8 model was built in Simulink to overcome the limitation introduced by the linearization of the state-space representation around a single flight condition. The block diagram of the 3-DOF simulator used to study the longitudinal motion of the plane is shown in figure 22.

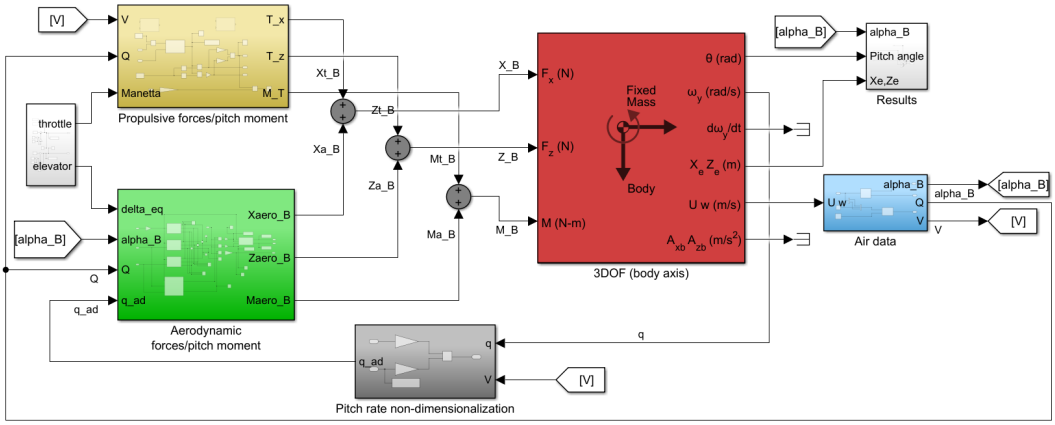

Figure 22 – Block diagram of the 3-DOF simulator implemented in Simulink

The dynamic model is based on three main blocks: two of them evaluate the aerodynamic (green) and propulsive (yellow) forces and moment, while the third one receives these ones as input and solve the 3-DOF equations of motion in body fixed axes. The outputs of the last block are then eventually used to calculate important flight variables and reconnected as inputs of the other two blocks. This block diagram allowed us to compare the dynamic response of the vehicle to a maneuver with the one expected from static analyses. In figure 23, as an example, the simulation starts in the statically defined conditions TRIM 1 (cruise) and, after 50s, a ramp command is executed with elevator and throttle (n_{thr}) to reach condition TRIM 2 ($\alpha_B = -3°, \gamma = 3°$) in 20s. Simulation results validate static analyses results, showing that the steady-state command response converges to the one statically predicted in TRIM 2.

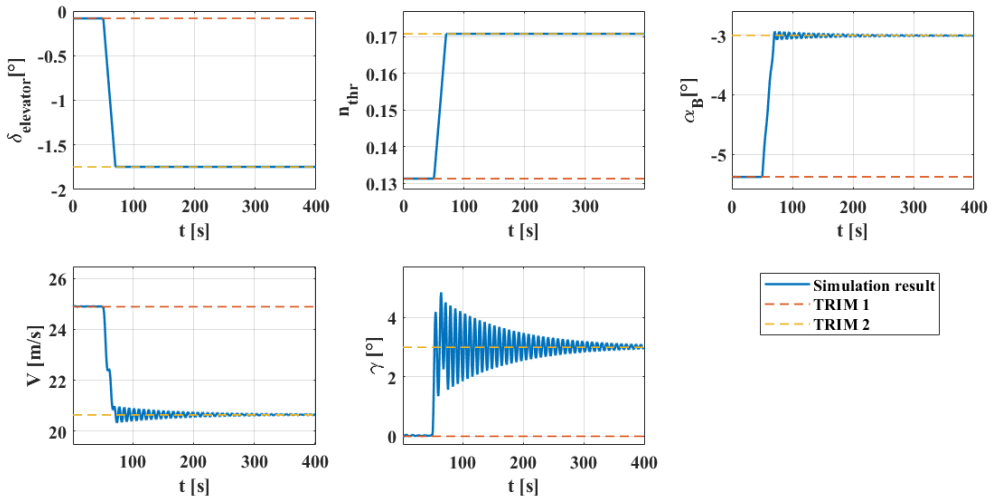

Figure 23 - Simulation results of a maneuver to change flight conditions from TRIM 1 to TRIM 2

5. FEM Analysis

5.1 FEM model

The structural analysis was made using the Finite Element Code ANSA [10], developed by BETA CAE System. The finite element idealization took place through the typical operations: the import of the CAD and geometry cleaning of all the errors, this operation is quite simple and the errors are due to a different resolution used by the programs for the two project phases; the choice of the surfaces to be used for 2D mesh (figure 24), the surfaces have been selected in order to simplify the next stages of modelling, for example: to be in contact with the interior elements, such as ribs, for hull and half-wing we used internal surfaces of the skins; lastly the choice of the components to be modelled in 3D and 1D through BEAM.

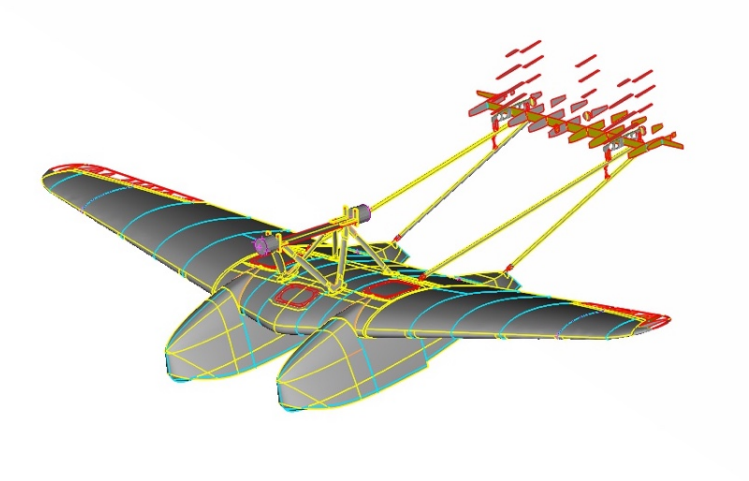

Figure 24 – The model after the geometry cleaning

The mesh was generated by creating various scenarios using the Batch Mesh command, through which it is possible to assign specific treatment and quality criteria to different parts of the model (figure 25).

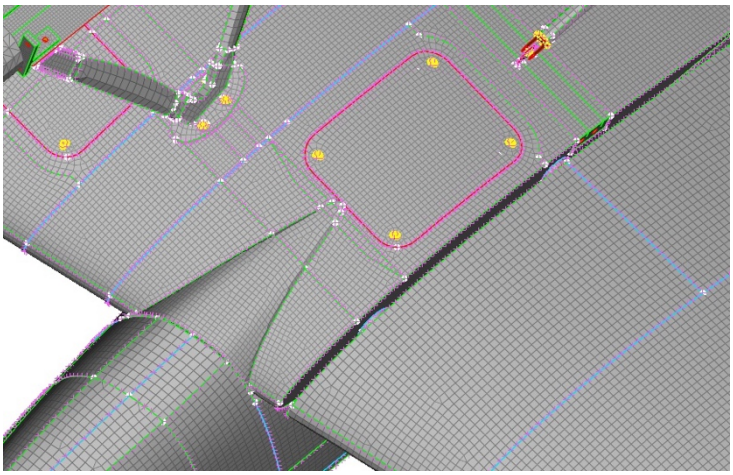

Figure 25 – Half-wing, Hull and Central Plane with their different mesh sizes

To lighten the model, the tail was shaped mainly with 2D and 1D beam elements, except for the rib made in additive manufacturing, shaped in 3D to have a more precise result (figure 26). Other components meshed with 3D elements are the engines (figure 27) and the spars where the ailerons are connected (figure 28).

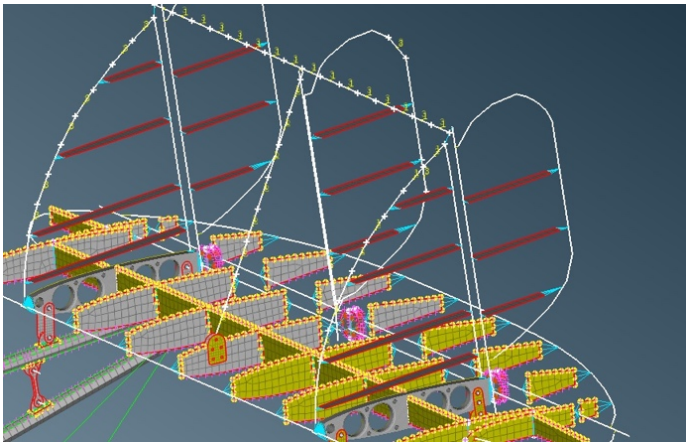

Figure 26 – Tail

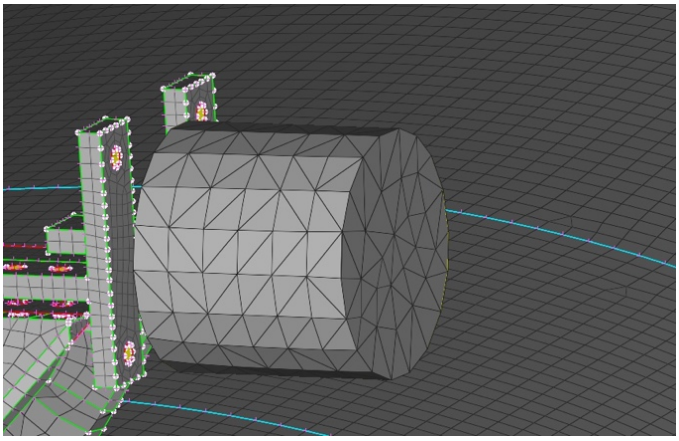

Figure 27 – Engine modeled with 3D elements

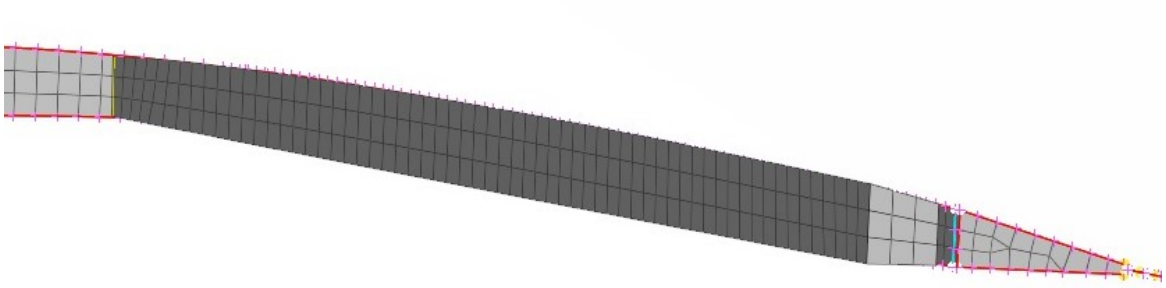

Figure 28 – Wing spar modeled with 3D elements

5.1.1 Materials

After the realization of the mesh, specific properties were generated for the laminates, assigned to the respective components and regions of the same component. Then we could generate a report for each property to see the sequence of the layers, their orientation (figure 29), and the resulting mechanical characteristics (figure 30).

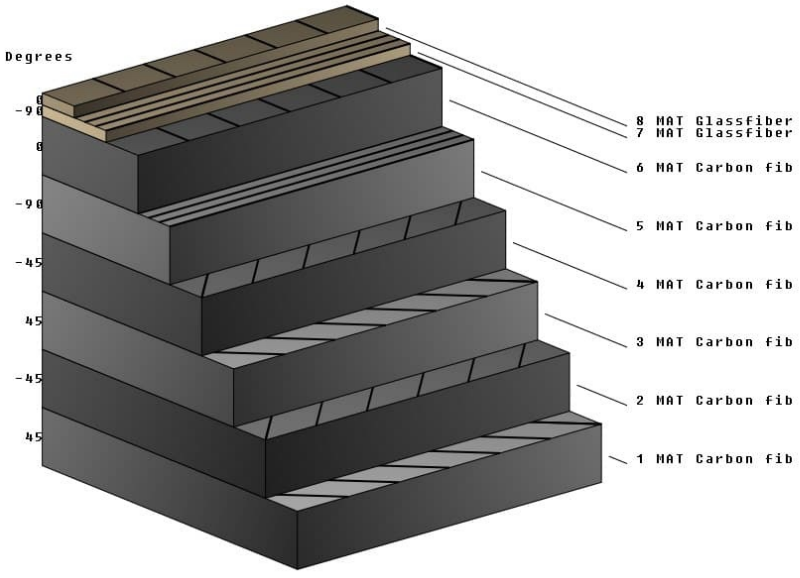

Figure 29 – Sequence of the layers of a laminate with their orientation

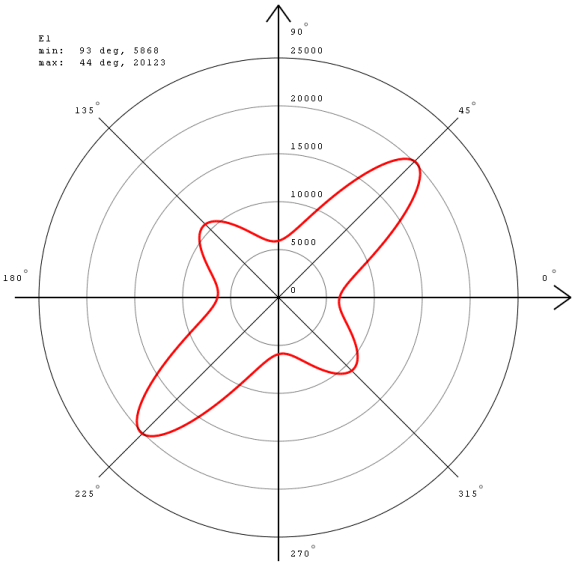

Figure 30 – Global Young Module of the laminate in direction 1 as a function of the angle

5.1.2 Connections and loads

For both the configurations, RBE2-BEAM-RBE2 are used to model screws and pins (figure 31); RBE2s are used to model the joints between the bayonets and the front longerons and between the sections of the rear ones.

For the loads we created a pressure load through PLOAD command (figure 32) and punctual forces, connected with RBE2 to the model, through FORCE command (figure 33).

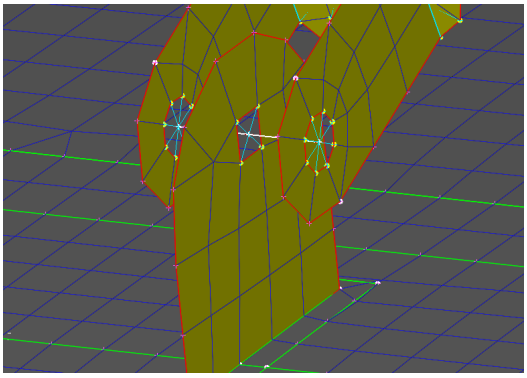

Figure 31 – RBE2-BEAM-RBE2 pin

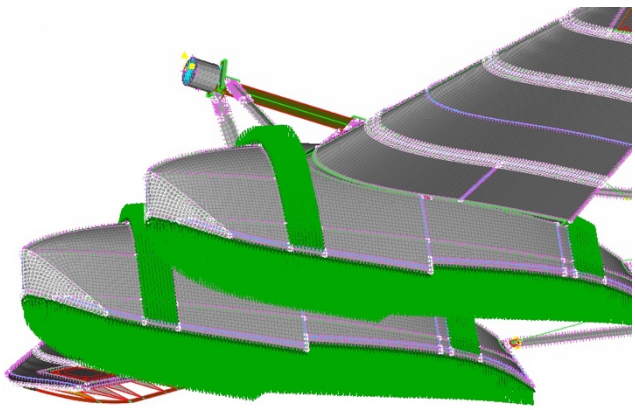

Figure 32 – Pressure loads applicated to the hulls

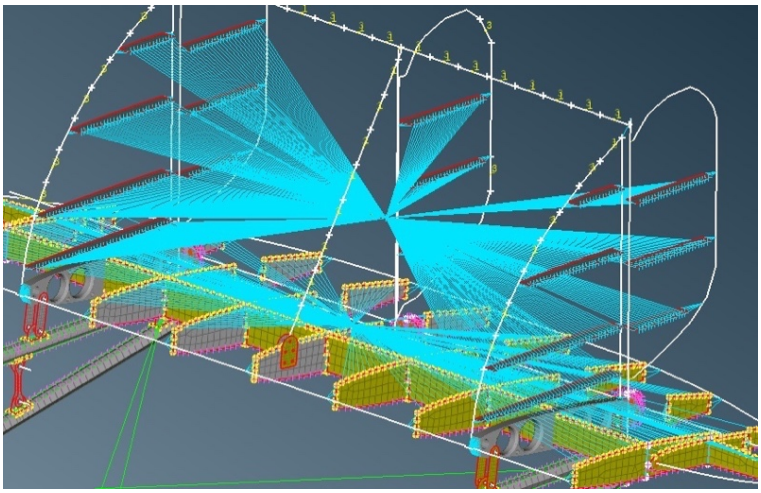

Figure 33 – Punctual forces connected with RBE2 to the tail

5.2 FEM results

5.2.1 Static analysis

In the first series of static analyses, inertial and aerodynamic loads were applied to simulate the ones to which the structure is subjected during flight maneuvers (pitch and yaw):

a) Pitch-Up with inertial loads on the hulls;
b) RH roll with inertial loads on the tail;
c) Pitch-Down with inertial loads on the tail;
d) A combination load between (b) and (c);
e) RH roll with inertial loads on the engine mount;
f) Horizontal impact in water with inertial loads on the engine mount;
g) Vertical impact in water with inertial loads on the engine mount;
h) A combination load between (e), (f) and (g);

In order to validate the finite element model, the first of the listed analyses was chosen as a reference to perform a static test in the laboratory whose results were very useful for evaluating the reliability of the model; in this simulation the constraints were located under the proper wing ribs while the loads were applied by pressure by means of load straps placed that are in the front and in the rear parts of two hulls (figures 34 and 35). The FEM calculated displacements are well predicting the static test results. The FEM theoretical stiffens is satisfactorily simulating the measured one in the test.

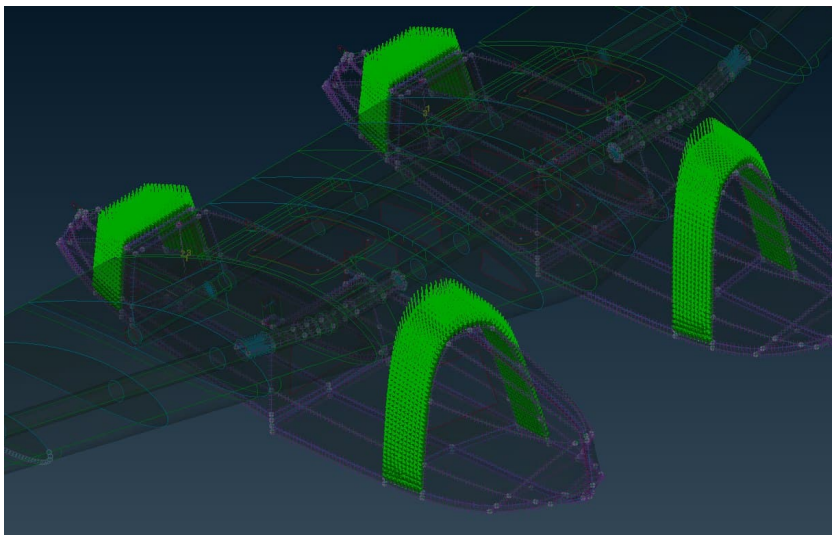

Figure 34 – The green arrows in the image show the area of the hulls in which the pressure loads are applied

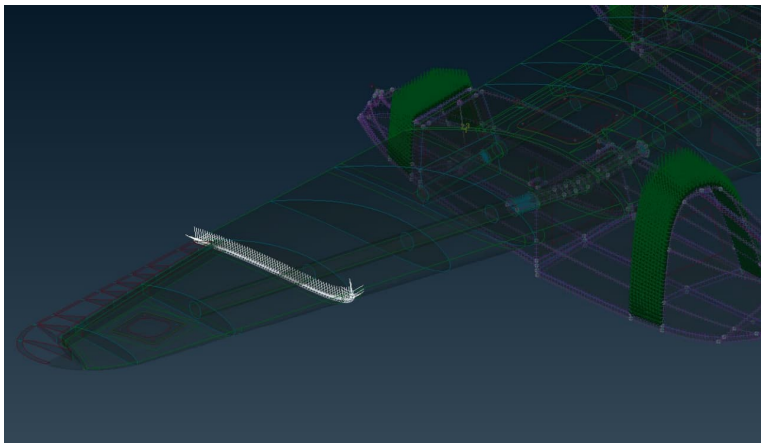

Figure 35 – The white points show the nodes constrained at the fourth rib of the right half-wing. There is the same constraint on the left half-wing

Other static analyses:

a) Vertical impact in water with pressure loads on hulls on both hulls (symmetrical case);
b) Ditching on a hull.

The results of the analysis show that the value and distribution of stress and strains are reasonable:

- The greatest stresses are located in the longerons and in the bayonet at the ribs in the interface area between the central plane and the half-wing;
- The deformations involve the wing in an almost homogeneous way as well as the structures subjected to the highest stress. The area that undergoes the most deformation is the rear side skin of the hull;
- Failure index is low except for the constraint zone.

5.2.2 Proposed modifications on the components

The structural analyses carried out on the various versions of the aircraft have, from time to time, provided for reinforcement solutions, where the resulting stresses were too close to the yield stress, and for lighter solutions for oversized components. Just consider the wing ribs and the hull frames for which 20% of the weight was saved.
Among the future steps of the structural analysis there will be a further study of lightening the aircraft to reduce the structural weight as much as possible.

6. Conclusions

In this study we wanted to make an overall analysis of the project carried out by the students of Team S55 of the Polytechnic of Turin. The main simplification steps that led to the creation of the aircraft CAD were analyzed, on which the construction with modern materials, was then based. The studies carried out by the Team on this CAD have been described, in order to have an optimal project from every point of view: structural, aerodynamic, materials and statics and dynamics of the aircraft. The fundamental point was the constant control of the weights and the position of the center of gravity, which allowed us to choose the best configuration for the installation of the system components, in order to have the center of gravity of the aircraft in the ideal position between the rear and front limits.
This experience gave us the opportunity to simulate the integrated activity of a real structural design team which includes teamwork, review meeting and project management. Grateful for the fantastic opportunity that has been given to us, we will continue to carry on our work by evolving and improving. The main purposes that Team S55 is determined to carry out in the immediate and near future are: flight tests of the complete 1: 8 scale model aircraft and the launch of the new S55 HERA (High Efficiency Replica model Aircraft) project. This new project will start from the completed model aircraft and will improve its efficiency through structural modifications with the study of a new geometry of the wings and modifications to the propulsion system with the study of a system based on hydrogen Fuel-

Cell technology. In this way we will want to retrace with the S55 HERA aircraft a range flight comparable to the historical crossings of the S55X.

7. Acknowledgments

The authors would like to thank the companies and people who contributed to this paper and to the 1:8 scale replica of the S55X. First of all, the entire Team S55, made up of young students full of enthusiasm, then Professor Enrico Cestino and engineer Vito Sapienza, who constantly support the project by making their experience and time available to the team. We would also like to thank the Politecnico di Torino which has been supporting the team financially since 2017 investing in our projects.
Last but not least, thanks to all the companies and organizations that collaborate with the S55 Team: Replica 55, Ellena-SPEM, BETA CAE Systems, Altair Engineering, HPC Polito, Siemens and Mike Compositi.

8. Contact Author Email Address

Mail to: teams55.polito@gmail.com

9. Copyright Statement

References

[1] http://replica55.it

[2] *“Istruzioni per il montaggio e per la regolazione - Idrovolante Savoia Marchetti tipo S.55X° I. F. Asso 750 serie 24+1 scafi allargatissimi per crocera” [ENGLISH: “Assembly and adjustment instructions - Savoia Marchetti seaplane type S.55X ° I. F. Asso 750 series 24 + 1 widened hulls for cruising”].* Ministero dell’aeronautica – Direzione generale delle costruzioni e degli approvvigionamenti, Società Idrovolanti Alta Italia – Sesto Calende

[3] *“Nomenclatore del materiale speciale d’aeronautica – Catalogo Nomenclatore per Idrovolante Savoia Marchetti tipo S.55X° I. F. Asso 750 serie 24+1 scafi allargatissimi per crocera” [ENGLISH: "Nomenclator of special aeronautical material - Catalog Nomenclator for Savoia Marchetti seaplane type S.55X ° I. F. Asso 750 series 24 + 1 widened hulls for cruising"]*. Ministero dell’aeronautica – Direzione generale delle costruzioni e degli approvvigionamenti, Società Idrovolanti Alta Italia – Sesto Calende

[4] *“Volume F4 – Flying Scale Model Aircraft”*. FAI Sporting Code, 2019 Edition

[5] *“T700S – Standard modulus carbon fiber*”. Toray Composite Materials America, Inc.

[6] *“Un approccio innovative per la produzione di stampi a basso costo” [ENGLISH: “An innovative approach to low cost mold manufacturing].* Iavecchia P, Maritano G, Loiodice L, Di Ianni L, Cestino E, Sapienza V and Frulla G. *Compositi Magazin*e, giugno 2020

[7] *“Additive manufacturing of composite tooling in RPAV production”*. Cestino E, Frulla G, Sapienza V, Di Ianni L, Iavecchia P, Maritano G, Ferrara M, Frisoli A and Michelotti A. AIDAA XXV International Congress, 9-12 September 2019, Rome – Italy

[8] http://web.mit.edu/drela/Public/web/avl/

[9] *“Simcenter Star CCM+ Documentation version 2020.1”*. Siemens Digital Industries Software

[10] https://www.youtube.com/channel/UCFMmoFjnrxZP4xf6-6GMquA